



***In silico* Screening and Identification of Inhibitor Molecules Targeting SDS22 protein**

RITIKA SAXENA^{1*} and SANJAY MISHRA²

¹School of Biotechnology, IFTM University, Moradabad, 244102, U.P. India.

²Department of Biotechnology, SR Institute of Management & Technology, Lucknow, 226201, U. P., India.

*Corresponding author E-mail: ritikashrivastava88@gmail.com

<http://dx.doi.org/10.13005/ojc/390315>

(Received: April 02, 2023; Accepted: May 23, 2023)

ABSTRACT

World's population is increasing at an alarming rate. Contraceptive methods for male are comparatively less common than female. Sperm motility, an indicator for fertilisation, is regulated by a set of proteins of protein phosphatase (PP) family. Among these PP1 is directly related with sperm motility. SDS22 (suppressor of Dis2 mutant 2) is a conserved and extensively expressed PP1 regulator, with less information regarding its function. This study used SDS22 protein from *Homo sapiens* as target and 100 plant-based compounds as the most relevant lead molecules with highest binding energy and affinity. Furthermore, this research incorporates homology modelling of SDS22 and protein-ligand interaction analysis. Benzeneacetonitrile, 4-hydroxy- had a binding energy of $-6.9 \text{ kcal mol}^{-1}$, higher to the reference MDP's $-3.5 \text{ kcal mol}^{-1}$, while other ligands exhibited binding energies of $-6.2 \text{ kcal mol}^{-1}$ for -terpineol, Coumarin, and 2-Phenylpropan-2-ol. These compounds may reduce the sperm motility and pave a promising path towards male contraception.

Keywords: Sperm motility, Male contraception, Protein-ligand interaction, SDS22, molecular docking.

INTRODUCTION

The phosphoprotein phosphatase (PPP) family consists of seven members that are present in all eukaryotic cells and contributes a significant amount of protein phosphatase activity to tissue extracts.¹ In vertebrates, 200 regulatory proteins regulate PP1 spatiotemporally, allowing for the creation of highly selective PP1 holoenzymes.² Primary role of PP1 regulatory proteins is to localize PP1 to a particular subcellular region, regulate catalytic activity, and/or facilitate substrate selection.

PP1 regulators may create trimeric PP1 complexes, which is intriguing.

PP1 γ 1 is present ubiquitously but PP1 γ 2 is only present in germ cells and spermatozoa.¹ PP1 γ 2 has been found to be present in most of the mammalian species and with an astounding similar structure, elucidating that this conservation is most likely related to sperm specific role in different species.³ Testis-specific PP1 γ 2 is crucial in the final stages of spermatogenesis⁴ and this is where the understanding mechanism of action of activation,



inhibition of PP1 γ 2 becomes crucial since PP1 γ 2 is not inhibited by the usual regulators of PP1 such as I1 and I2. The activity of PP1 γ 2 phosphatase has been shown to be negatively connected with motility, i.e., Low activity in caudal spermatozoa that are actively moving and high activity in caput spermatozoa that are not moving.⁵ Previous studies have isolated an inactive complex of PP1 γ 2-SDS22 from caudal sperm whereas catalytically active PP1 γ 2 has been isolated from caput sperm. It could be inferred that this binding with SDS22 and subsequent inactivation of PP1 γ 2 is one of the major steps in maturation of spermatozoa.^{6,7}

SDS22 (also known as PPP1R7) is a PP1 regulatory component that is mainly preserved among bovine, human and mouse orthologs.^{8,9} There are 360 residues in human SDS22, with twelve leucine-rich repeats (LRRs) predicted. An LRR cap that flanks SDS22 LRRs on the C-terminus is thought to shield the LRRs' hydrophobic core from solvent.¹⁰ SDS22 and PP1 and Inhibitor-3 may combine to produce heterotrimeric complexes^{9,11} or KNL112, indicating that SDS22 and Inhibitor-3/KNL1 have PP1-binding sites that at least partially overlap one another.

Despite the fact that one of the most prevalent and conserved PP1 regulators is SDS22,¹³ little is known about its function. PP1:SDS22 has also been linked to chromosomal segregation^{12,14} and cell shape control.¹⁵ SDS22 decreases the catalytic activity of PP1 γ 2 which in turn enhances the motility of sperm.^{9,16} Recent findings suggest that SDS22 regulates various stages of PP1's life cycle. It is involved in stabilization, translocation and storage of PP1.¹⁷ PP1 that has been discharged or has grown old may also be scavenged by SDS22, which can be used again in holoenzyme assembly or proteolytic destruction, according to preliminary findings.^{18,19}

SDS22 is located on chromosome 2q37.3, and been found to be one of the most often deleted areas in various malignancies, and mostly inactive owing to loss of heterozygosity.²⁰ It has been revealed to be a crucial regulator of the G2/M cell cycle progression in previous investigations.^{21,22,23} It has also been linked to chemo-resistance in ovarian cancer.²⁴

Computer-aided drug design (CADD) and in silico pharmacotherapy are expanding fields that involve the development of software tools for gathering,

evaluating, and mixing facts about biology and medicine from several sources.²⁵ Therapeutic agent screening has been facilitated by the pharmaceutical sciences and other academic fields, with rapid high-throughput results.²⁶ Furthermore, by supplying a richer understanding of the target-receptor interaction, bioinformatics tools offer a better comprehension of the biological effect.^{27,28} Identification of prospective medication compounds entails a sequence of steps, starting with illness selection, then selecting an appropriate target molecule, building a small molecule library, and scoring research on target-ligand interactions. The technique of "molecular docking" foretells the connection between the protein and the ligand, in addition it also tells the ways in which the ligand and protein interact.^{29,30} Although molecular docking is a quick method for figuring out how any ligand will attach to a protein's active site, the outcomes have several drawbacks. As a result, as the system is simulated under temperature fluctuations, simulation is followed by docking to mimic the natural biological systems.³¹

This study consolidates the homology modelling of SDS22 protein followed by molecular docking, molecular dynamics and protein-ligand interaction analysis. Hence, this study included SDS22 protein of *Homo sapiens* as a target protein, and 100 plant-based compounds were selected to determine suitable lead molecule having highest affinity and binding energy to understand and elucidate the mechanism of motility inhibition of spermatozoa using in silico studies.

MATERIALS AND METHODS

Homology modelling of protein

In order for our body's basic functions to be carried out completely, the choice of protein and ligand is crucial to the CADD process as a whole. The protein sequence database was used to acquire the SDS22 amino acid sequence, i.e., UniProt.³² The retrieved sequence was then searched to obtain modeling templates using the Protein-BLAST program.³³ The template with the highest sequence similarity and query coverage were then selected. A selected template was 'Okadaic acid, a tumor-promoting substance, is linked to protein phosphatase-1 in the crystal structure. (PDB ID:1JK7)' as template structure showing 100% sequence identity and 93% query coverage with

PP1 γ 2 sequence. The three-dimensional protein structure of SDS²² was then predicted using Phyre2, followed by a comparison with the available models in the Protein Model Portal³⁴ predicted through MODBASE³⁵ and SWISS-MODEL.³⁶

Model Validation and Optimization

The Models generated for SDS²² used two different homology modeling approaches, and the ab-initio prediction was then validated using different methods. The optimisation of the model is a suitable method for correcting errors and carrying out energy minimization because a predicted model can contain some small inconsequential flaws and high energy configurations, likely causing a physical disruption and instability of the structure. The model's energy consumption was reduced utilizing the Swiss PDB viewer (SPDBV) tool.³⁷ In order to accurately simulate the structure of a protein, model evaluation and validation are crucial steps. Evaluation for generated models of SDS²², SAVES servers (Structure Analysis and Verification Server) that collectively checked model in several independent programs, including ERRAT, Verify 3D³⁸, Prove, Procheck, ProSa, ProQ and RAMPAGE³⁹. For predicting overall model quality in terms of total energy deviation of protein, Z-score was estimated using ProSA web server. To further check accuracy of the protein structure Ramachandran Plot was generated using Discovery Studio⁴⁰, which supports the appropriateness of the predicted model.

Phytochemical ligand library preparation

Phytochemical compounds were selected as potential lead molecules to dock against the target protein, SDS²². Since ancient times plant-based compounds have been in the limelight for their immense potential as antibacterial and antiviral agents. Such 100 plant-based compounds were selected, and their structures were obtained from PubChem (<https://pubchem.ncbi.nlm.nih.gov>), including information on their structure, characteristics, and uses. Phytochemicals were acquired in SDF format and converted using Open Babel into PDB files.

Drug-likeness property analysis of ligand

To determine the cytotoxic activity of compounds, a drug-likeness calculation was carried out for humans by DruLiTo open-source software. Based on specific physiochemical and structural

characteristics, a ligand's drug bioavailability or drug-likeness defines its pharmacological significance. Consequently, using Lipinski's rule of five, all ligands were assessed for their potential as drugs⁴¹ by DruLiTo software. The suitable file format for DruLiTo is .sdf, first 100 molecule structures obtained from the database were merged to a single .sdf file using the OpenBabel file format converter. The combined file was then uploaded on the page of DruLiTo, the sole filter used to screen the molecules was the Lipinski rule of 5. The calculated properties obtained were then exported as a .csv file to the desired folder. Structure of molecules that made it through the filter was then saved from the file-save Lipinski filtered molecule option.

Protein and Ligand preparation

3D structure of protein SDS²² model was generated and then got ready for docking. The protein molecule was stripped of all ligands, ions, and water molecules using PyMOL software for preparation. After adding hydrogen atoms to the receptor, the molecular docking was accomplished using MG Tools of AutoDock Vina software.⁴² The protein structure was then stored in PDB format for later study. Before starting the docking procedure, using the "centre of mass" command line in PyMOL software to get the x, y, and z coordinates of the reference molecule and for all the proteins, the centre of mass of the co-crystallized ligand was examined. These coordinate sites were their active site. The coordinate sites of the protein SDS²² were (-2.13, 24.63, -9.66). The ligands used for the docking process are prepared before using them. The success of the docking process depends on choosing and processing the coordinates for receptors and ligands correctly. Therefore, the qualities of the coordinates in ligand and protein have significance in this process. To complete these preparation steps, the .pdb file format needs to be changed to the PDBQT file format. All water molecules were removed, and ADT software was used for preparing the necessary files for AutoDock Vina allocating hydrogen polarities, calculating Gasteiger and Kollman charges to protein and ligand structures.^{43,44,45}

Molecular Docking study

Using Autodock Vina, a molecular docking procedure was carried out into the SDS²² domain's active site⁴² under PyRx (an open-source software-

GUI version 0.8 of autodock). Autodock Vina and PrRx are docking tools that employ the target protein's atomic structure along with the ligand of choice, and also predict which docking conformation between the two will work best. X-ray Crystallography and NMR Spectroscopy accessed the target protein coordinates, whereas ligand molecules were obtained in the Structure-Data file (.sdf) from the PubChem database. One simplification method that Autodock Vina uses is considering receptors as rigid molecules. Therefore, it reduces the size of the conformational space search, making the process reliable and less time-consuming as scoring of each trial confirmation is not done. Forcefield used for the study was a Physical based method that included directional hydrogen bonding, primarily polar hydrogen and electrostatics.

Preparation of coordinates files was performed as described, and after preparation of the required files, each of the files was closely observed for their protonation state and their charges. The metal-bound state was checked for its information compatibility with the existing knowledge. As ADT does not provides charges to the bound metal ion. Therefore, this has to be added manually to a text document. So, a text editor was used to directly add the prepared PDBQT file. Proteins prepared by adding missing hydrogens were loaded on the page of AutoDock Vina, and a grid box point each for SDS22 proteins in x, y, and z directions were built according to their coordinate site with a grid spacing of 25 Å°. Vina configuration file was then generated on a text document named conf.txt. The configuration file for each ligand was prepared with the mentioned coordinates(-2.13, 24.63, -9.66), grid box size ≈25, and grid spacing of 25 Å°. The target (protein) was kept rigid during the docking process, while ligands were flexible in determining the most suitable pose. The command line was used to run Autodock Vina. The directory containing the protein and ligand files were accessed, commands were run. Vina_split and vina.exe were also kept in the same directory.

In the case of PyRx (an open-source software-GUI version 0.8 of autodock), protein and ligand preparation steps were performed in the program omitting the need for preparation on the ADT platform. PDBQT files were generated, and then the grid box was adjusted to the position of the active site in all three proteins. All the ligands were loaded in

the same panel, and the autodock program was run. The resultant files automatically get saved to the mgl tools that can be determined/edited from the EDIT-Preferences option of the main menu. The output of the autodock run using the PyRx program can be visualized by opening the pdbqt file of a target protein and the pdbqt of ligands obtained after running. To observe the binding of a small molecule inside the protein pocket, a right-click on the protein name on the left-hand side options panel shows an option of Display and then molecular surface. In contrast, the ligand molecule must be displayed in ball and stick form to visualize the docked molecule. All the poses of the same molecule and different poses of several molecules can be superimposed to compare their binding in the protein's active site pocket.

Protein-ligand interactions

The highest-ranking postures were chosen following the docking procedure for additional protein-ligand interaction investigation. The interaction was shown using the application LigPlot+ v.1.4.5. This tool makes it easier to translate 3D structure into a 2D picture, allowing thorough investigation of the 2D hydrogen and hydrophobic interactions within the protein-ligand complex.

The resultant binding energies were observed from the log file of each ligand (small molecule). Based ligands were screened from the results, filtering out others. Each ligand's output (in pdbqt format) file contained all the poses in one file. Among these poses, after identifying the top-scoring molecules and their highest-ranking pose, poses were split to obtain separate structures of each molecule. First, splitting was done by copying the three vina files (vina, vina_license, and vina_split) in the directory containing the output of docking results. Then using the cmd prompt, the following command was run to obtain a split file.

The separated poses for each ligand were then obtained in the same folder. The output pdbqt file was then opened on LigPlot+ v.1.4.5 along with the pdbqt of protein to observe an interaction between residues of protein and ligand. The interaction between the most suitable ligand and protein observed on LigPlot was subsequently examined to determine the acting amino acid residues in the protein's active site, type of bonds formed between residues and atoms of ligand, and

bond length. The recorded data were then compared with the reference molecules and their interactions with the target protein.

RESULTS

Homology modelling

Three hundred sixty amino acid residues make up SDS22, which has a molecular weight of 41,564 Da (about 42 kDa). The three-dimensional protein structure of SDS22 was predicted using Phyre2, followed by a comparison with the available models in the Protein Model Portal³⁴ predicted through MODBASE³⁵ and SWISS-MODEL.³⁶ The predicted model was aligned with 2.44Å and 0.75Å RMSD with MODBASE and SWISS-MODEL models, respectively, supporting the prediction and reliability of the modeled structure (Figure 1).

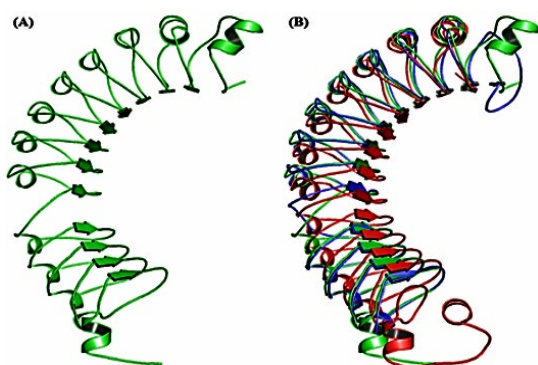


Fig. 1. Cartoon representation of SDS22. (A) Predicted model of SDS22 using Phyre2 and (B) Superimposition of aligned models predicted through Phyre2 (Green salmon color), MODBASE (Red salmon color) and SWISS-MODEL (Light-Blue color)

Model Optimization

This study checked and evaluated the model using several bioinformatics tools and servers of SAVES (Structure Analysis and Verification

Server), including ERRAT, Verify 3D³⁸, PROVE, and PROCHECK. Along with this server PROSA, PROQ and RAMPAGE tool were also employed to evaluate the protein structure's quality. Results from all the tools deciphered that the predicted structure is accurate and will remain stable during biological processes (Table 1). In the predicted model of SDS22, 72.3% residues are present in the most favored region, 26.2% residues were present in the allowed region and 1.5 % residues were found in the generously allowed region and 0.0 % of total protein, are present in the disallowed region demonstrating that the anticipated model of SDS22 is of a suitable quality (Figure 2).

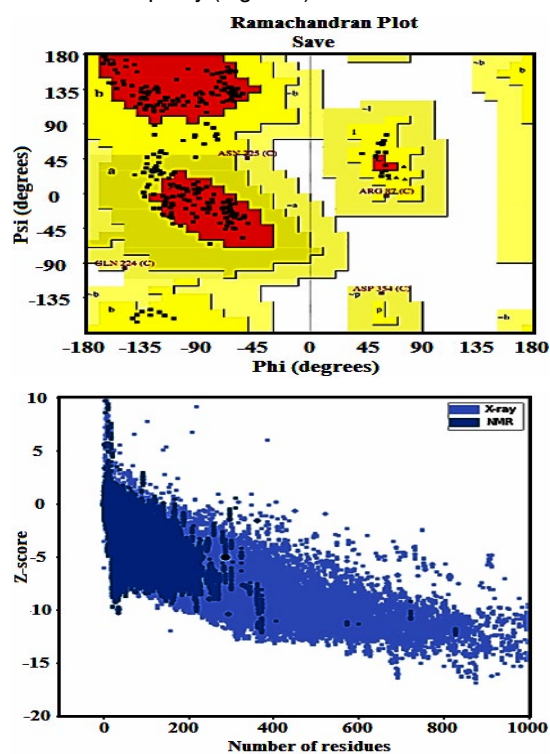


Fig. 2. Ramachandran Plot and the Z Score Calculation of the modelled protein

Table 1: Model Validation using the various model analysis tool

	VERIFY1 3D	ERRAT2	PROVE3	PROCHECK4	PROSA5	PROQ6	RAMPAGE7
Model SDS22	96.14Pass	77.978	1.487	E:2W:2P:4	-5.03	9.298	-98.5%~1.5%~0%

¹3D score \geq 0.2 is required for no less than 80% of the amino acid residues.

²It describes the quality factor of the modelled protein structure.

³The quality of a structure can be predicted using Voronoi Radical planes.

⁴Describe the accessible Error Warning and Pass of predicted structure.

⁵Z Score is used to predict the model structure's quality.

⁶In terms of LG score, the quality of the simulated score is projected.

Active site prediction

Accurate prediction of the active site before docking is essential in bioinformatics⁴⁶. Thus, coordinate locations of the active site of

protein were calculated using the "centrofmass" and VMD process, as mentioned earlier. The coordinate sites of the protein was found to be -2.13, 24.63, -9.66.

Construction of phytochemical library

In view of less studied phytochemicals from plants as potential lead molecules against SDS22, our study explored 100 small molecules of plant origin to identify their binding affinity for the selected protein. Following the selection of 100 small plant compounds from the PubChem database based on their properties, the SDF files for all 100 molecules were retrieved from the same database. Lipinski's rule of five is employed to determine in humans the best way to deliver a medication orally⁴⁷. Using Open Babel, the SDF data of these 100 molecules were translated to PDB files, then DruLito software was utilized to screen the molecules, which identified 28 molecules that was suitable for lead compounds since it adhered to the Lipinski rule of five.

Molecular Docking Analysis

The starting of a docking study is marked by defining a specific protein region called the binding site, into which small molecular compounds are docked, and their affinity is estimated, and this contributes a significant region of the protocol of designing drug based on structure.⁴⁸ Out of 100 possible phytochemicals, docking studies for the molecular target SDS22 revealed that five had greater binding affinities and binding modes than the reference (MDP). For further study, the 2D structures of the selected phytochemicals were acquired.

The binding energy of molecular targets, SDS22, with six compounds is shown in Table 2. Predicting the affinity of a ligand's binding is a crucial step in the CADD procedure⁴⁹, where the binding equilibrium free energy between two molecules is used to define the binding affinity.⁵⁰ In the case of SDS22, Benzeneacetonitrile, 4-hydroxy- showed -6.9 kcal mol⁻¹ binding energy which was closest to reference MDP with -3.5 kcal mol⁻¹ while other ligands had binding

energies of -6.2 kcal mol⁻¹ for -terpineol, -6.2 kcal mol⁻¹ for Coumarin, -6.2 kcal mol⁻¹ for 2-Phenylpropan-2-ol and -6.0 kcal mol⁻¹ for Alpha citral. Comparing all phytochemicals to reference compounds, they all displayed somewhat lower binding energies. These five phytochemicals are therefore effective at inhibiting these molecular targets.

Ligand and Receptor Interaction

The molecular target protein and many phytochemicals that were assessed combined 2D interactions that were examined using hydrogen bonding sites with references and hydrophobic interactions with various residues, shown in Fig. 3. In the figures, the reference molecules are depicted in green, and the screened phytochemicals are shown in purple. Several molecular targets had distinct standard binding sites. In the figures, the red sparking arcs depict residues creating hydrophobic interactions with phytochemicals, while the green dotted lines represent hydrogen bonds with limitations. Protein residues in equivalent 3D positions are denoted by red circles and ellipses.

The results demonstrated lower interaction numbers due to the cleaning step in LigPlot+, which is the step before plotting, which minimizes the number of overlapping atoms and bonds to provide a possibly clear outcome of ligand interaction. Table 2 represents the interacting amino acids of SDS22 protein with selected ligands. The treatment given to the hydrogen and hydrophobic bonds are not similar, i.e., all-atom in the side chains are kept in the group with hydrogen bonds; also, atom of the main chains can also be kept whereas, a single spot is demonstrated for hydrophobic ones, linking to ligand atom via a virtual bond. The interactions were also visualized by using Discovery Studio to get a clearer picture of the interactions (Figure 4).

Table 2: Protein Ligand Interaction Analysis

S. No	Ligand Name	Binding Energy Kcal mol ⁻¹	Interacting Residues	H Bond Donor	H Bond Acceptor	H Bond Distance
1	Reference (MDP)	-3.5	ARG340 TYR339	2.40827 2.21981	HN HN	O2 O4
2	Benzeneacetonitrile, 4-hydroxy	-6.9	TYR339 ARG340	2.36572 2.26533	HN HH12	O O
3	α -Terpineol	-6.2	ARG340 THR356 GLN334	2.1115 2.42985 2.1794	HN HG1 H	O O O
4	Coumarin	-6.2	ARG340 THR356	2.17832 2.439	HN HG1	O O
5	2-Phenylpropan-2-ol	-6.2	ARG340 THR356 THR356	2.23012 2.06002 2.01156	HN HG1 H	O O OG1
6	Phenanthridone	-6	TYR339 ALA355 THR356 PRO337 THR356	2.16812 2.15701 2.36301 2.37724 2.27078	HN HN HN H H	O O O O OG1

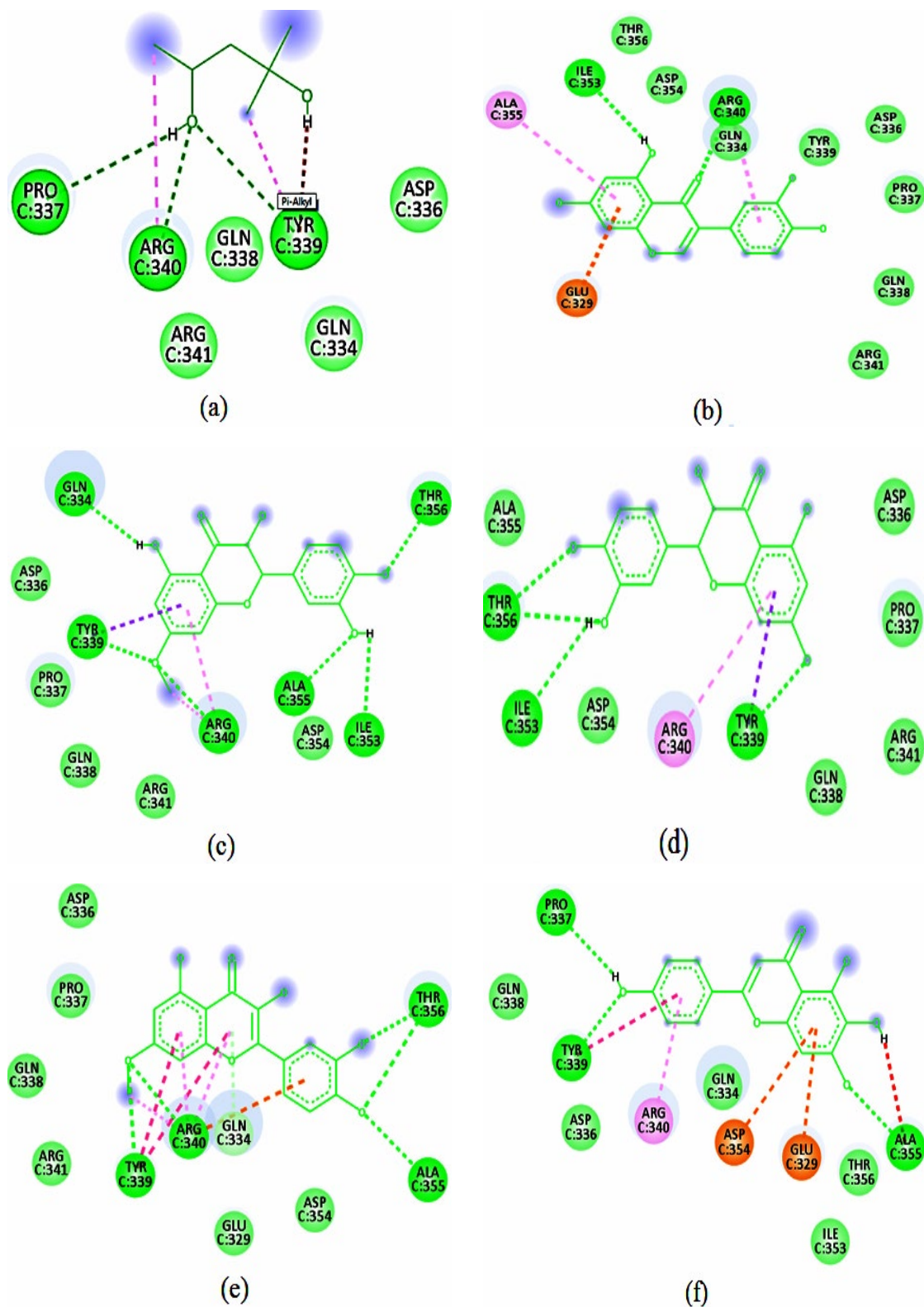


Fig. 3. 2D Interaction analysis of SDS22 protein and the ligand compound

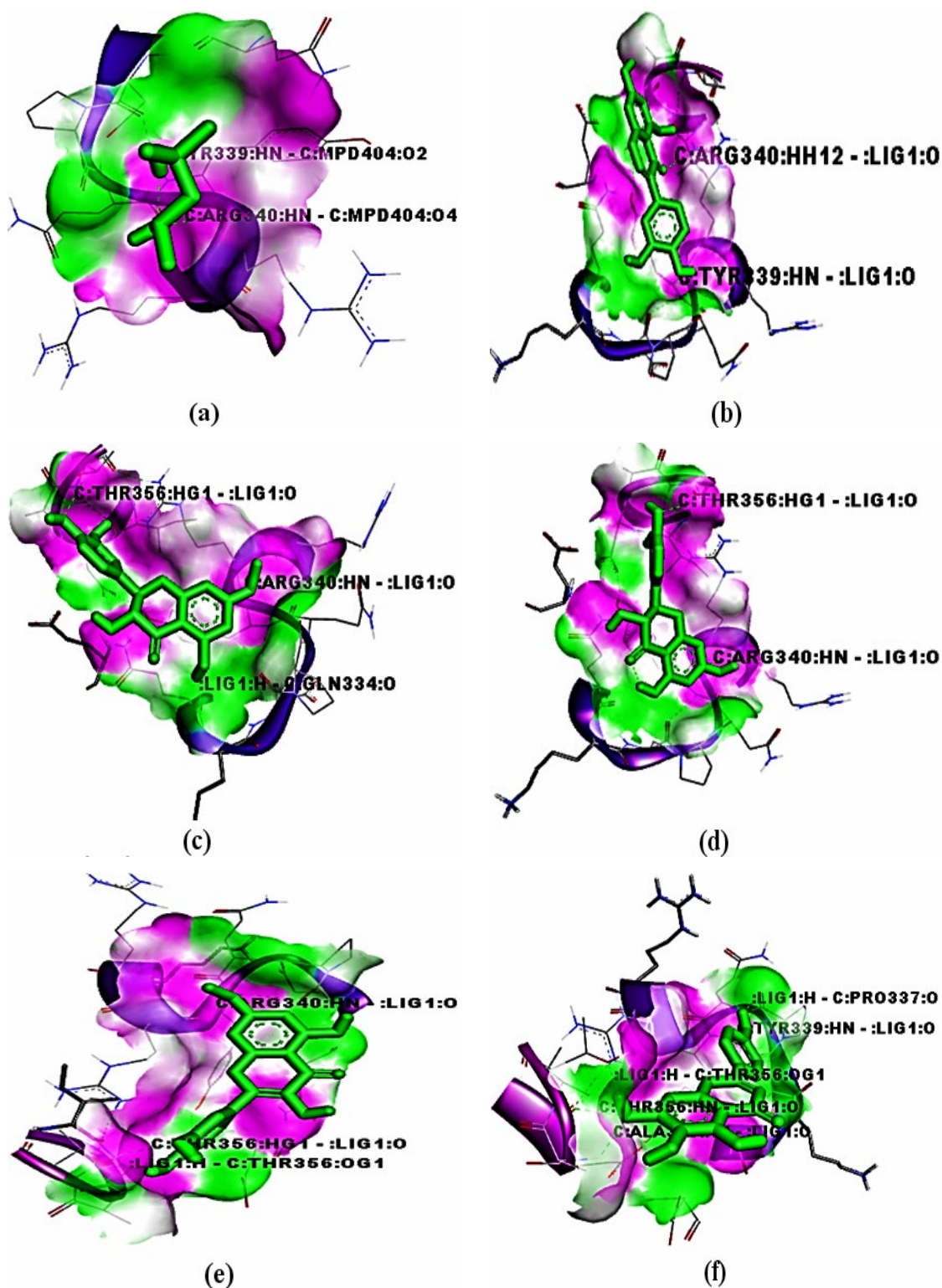


Fig. 4. SDS22 Protein-Ligand interaction analysis (a) Reference, (b) Benzeneacetonitrile, 4-hydroxy-, (c) α -Terpineol, (d) Coumarin, (e) 2-Phenylpropan-2-ol, and (f) Alpha citral. Poses show ligands in sticks (green). Residues with potential interactions are shown as sticks with protein, and bonds as dotted yellow lines

DISCUSSION

The SDS22 protein from *Homo sapiens* was employed as a target protein in this study, and to identify the most pertinent and significant lead molecule with the highest binding energy and affinity, 100 plant-based compounds were selected. Computational biology pipeline was followed to study the library of medicinal active compound and perform the druglikeness activity. Promising compounds were docked with SDS22 protein. From the docking analysis study, 5 compounds from the pool of library were selected and their interaction analysis was performed. The criteria for the analysis of interaction were binding energy, H-bond distance and the interacting atom. The identified compounds were having the good binding energy along with the other criteria. Furthermore, this work combines homology modelling of the SDS22 protein with the molecular docking and protein-ligand interaction analysis. Thus, the study concluded that Benzeneacetonitrile, 4-hydroxy- had binding energy of -6.9 kcal/mol, which was closest to the reference MDP with -3.5 kcal mol⁻¹, while other ligands had binding energies of -6.2 kcal mol⁻¹ for -terpineol, -6.2 kcal mol⁻¹ for Coumarin, -6.2 kcal mol⁻¹ for 2-Phenylpropan-2-ol.

CONCLUSION

This study was targeted to identify potential inhibitors of SDS22 protein. This protein is a well-known regulator of PP1 γ 2 which mediates the activity of the sperm motility. In the study out of 100 compounds, on the basis of binding energy five compounds were selected among which Benzeneacetonitrile, 4-hydroxy- had maximum binding energy, i.e., -6.9 kcal mol⁻¹ and thus could be used to control sperm motility by acting as a potential inhibitor of SDS22 protein.

Due to the shortcomings of available male and female contraceptive methods, this study could be a new approach for male contraception. To substantiate these results, nevertheless, *In vitro* tests and molecular dynamics simulations are needed.

ACKNOWLEDGEMENT

Authors are thankful to School of Biotechnology, IFTM University Moradabad for providing the research facility.

Conflict of interest

The authors claim to have no conflicts of interest.

REFERENCES

- Dudiki, T.; Joudeh, N.; Sinha, N.; Goswami, S.; Eisa, A.; Kline, D.; Vijayaraghavan, S. *Biol. Reprod.*, **2019**, *100*(3), 721-36.
- Kokot, T.; Köhn, M. *J. Cell Sci.*, **2022**, *135*(19), jcs259618.
- Silva, J.V.; Freitas, M.J.; Santiago, J.; Jones, S.; Guimarães, S.; Vijayaraghavan, S.; Publicover, S.; Colombo, G.; Howl, J.; Fardilha, M. *Fertil. Steril.*, **2021**, *115*(2), 348-62.
- Dey, S.; Brothag, C.; Vijayaraghavan, S. *Front. Cell Dev. Biol.*, **2019**, *7*, 341.
- Serrano, R.; Garcia-Marin, L.J.; Bragado, M. *J. Biology.*, **2022**, *11*(5), 659.
- Bheri, M.; Mahiwal, S.; Sanyal, S.K.; Pandey, G.K. *FEBS J.*, **2021**, *288*(3), 756-85.
- Huang, Z.; Khatra, B.; Bollen, M.; Carr, D.W.; Vijayaraghavan, S. *Biol. Reprod.*, **2002**, *67*(6), 1936-42.
- Lesage, B.; Beullens, M.; Pedelini, L.; Garcia-Gimeno, M.A.; Waelkens, E.; Sanz, P.; Bollen, M. *Biochem.*, **2007**, *46*(31), 8909-19.
- Kern, C.H.; Yang, M.; Liu, W.S. *Biol. Reprod.*, **2021**, *105*(2), 290-304.
- van den Boom, J.; Meyer, H.; Saibil, H. *bioRxiv.*, **2022**, *26*, 2022-06.
- Pedelini, L.; Marquina, M.; Arino, J.; Casamayor, A.; Sanz, L.; Bollen, M.; Sanz, P.; Garcia-Gimeno, M.A. *J. Biol Chem.*, **2007**, *282*(5), 3282-92.
- Eiteneuer, A.; Seiler, J.; Weith, M.; Beullens, M.; Lesage, B.; Krenn, V.; Musacchio, A.; Bollen, M.; Meyer, H. *EMBO J.*, **2014**, *33*(22), 2704-20.
- Matos, B.; Howl, J.; Jerónimo, C.; Fardilha, M. *Drug Discov.*, **2021**, *26*(11), 2680-98.
- Fréville, A.; Gnangnon, B.; Treppe, A.Z.; De Witte, C.; Cailliau, K.; Martoriati, A.; Aliouat, E.M.; Fernandes, P.; Chhuon, C.; Silvie, O.; Marion, S. *Open Biol.*, **2022**, *12*(8), 220015.
- Rodrigues, N.T.; Lekomtsev, S.; Jananji, S.; Kriston-Vizi, J.; Hickson, G.R.; Baum, B. *Nature.*, **2015**, *524*(7566), 489-92.

16. Kern, C.H.; Feitosa, W.B.; Liu, W.S. *Front. Genet.*, **2022**, 13, 354.
17. Cao, X.; Lemaire, S.; *Bollen, M. FEBS J.*, **2022**, 289(11), 3072-85.
18. Mehta, V.; Chamousset, D.; Law, J.; Ooi, S.; Campuzano, D.; Nguyen, V.; Boisvert, F.M.; Moorhead, G.B.; Trinkle-Mulcahy, L. *bioRxiv.*, **2022**, 2022-09.
19. Troyanovsky, R.B.; Indra, I.; Kato, R.; Mitchell, B.J.; Troyanovsky, S.M. *J. Biol. Chem.*, **2021**, 297(5).
20. Takemiya, A.; Ariyoshi, C.; Shimazaki, K.I. *Plant Physiol.*, **2009**, 150(1), 144-56.
21. Chen, A.; Ulloa Severino, L.; Panagiotou, T.C.; Moraes, T.F.; Yuen, D.A.; Lavoie, B.D.; Wilde, A. *Nat. Commun.*, **2021**, 12(1), 2409.
22. García-Gimeno, M.A.; Muñoz, I.; Ariño, J.; Sanz, P. *J. Biol. Chem.*, **2003**, 278(48), 47744-52.
23. Bharucha, J.P.; Larson, J.R.; Gao, L.; Daves, L.K.; Tatchell, K. Yp1. *Mol. Biol. Cell.*, **2008**, 19(3), 1032-45.
24. Cheng, Y.L.; Chen, R.H. *J. Cell Sci.*, **2015**, 128(6), 1180-92.
25. Gurung, A.B.; Ali, M.A.; Lee, J.; Farah, M.A.; Al-Anazi, K.M. *BioMed Res. Int.*, **2021**.
26. Joseph, T.L.; Namasivayam, V.; Poongavanam, V.; Kannan, S. "Chapter 1: In silico approaches for drug discovery and development." Bentham Science Publishers., **2017**, 3, 3-74.
27. Sabe, V.T.; Ntombela, T.; Jhamba, L.A.; Maguire, G.E.; Govender, T.; Naicker, T.; Kruger, H.G. *Eur. J. of Med. Chem.*, **2021**, 224, 113705.
28. Xiao, X.; Min, J.L.; Lin, W.Z.; Liu, Z.; Cheng, X.; Chou, K.C. *J. Biomol. Struct. Dyn.*, **2015**, 33(10), 2221-33.
29. Jenardhanan, P.; Panneerselvam, M.; Mathur, P.P. *Molecular Mechanisms in Spermatogenesis.*, **2021**, 205, 14.
30. Sethi, A.; Joshi, K.; Sasikala, K.; Alvala, M. "Chapter 3: Molecular Docking in Modern Drug Discovery: Principles and Recent Applications." Drug Discovery and Development-New Advances [Internet]. *Intech Open, London, United Kingdom.*, **2019**, 2, 1-21.
31. Khan, K.M.; Rahim, F.; Wadood, A.; Kosar, N.; Taha, M.; Lalani, S.; Khan, A.; Fakhri, M.I.; Junaid, M.; Rehman, W.; Khan, M. *Eur. J. Med. Chem.*, **2014**, 81, 245-52.
32. UniProt Consortium. *Nucleic Acids Res.*, **2013**, 41(D1), D43-D47.
33. Altschul, S.F.; Gish, W.; Miller, W.; Myers, E.W.; Lipman, D.J. *J. Mol. Biol.*, **1990**, 215(3), 403-10.
34. Arnold, K.; Kiefer, F.; Kopp, J.; Battey, J.N.; Podvinec, M.; Westbrook, J.D.; Berman, H.M.; Bordoli, L.; Schwede, T. *J. Struct. Funct. Genomics.*, **2009**, 10, 1-8.
35. Pieper, U.; Eswar, N.; Webb, B.M.; Eramian, D.; Kelly, L.; Barkan, D.T.; Carter, H.; Mankoo, P.; Karchin, R.; Marti-Renom, M.A.; Davis, F.P. *Nucleic Acids Res.*, **2009**, 37(suppl_1), D347-54.
36. Schwede, T.; Kopp, J.; Guex, N.; Peitsch, M.C. *Nucleic Acids Res.*, **2003**, 31(13), 3381-5.
37. Guex, N.; Peitsch, M.C., *Electrophoresis.*, **1997**, 18(15), 2714-23.
38. Bowie, J. U.; Luthy, R.; Eisenberg, D. *Science.*, **1991**, 253(5016), 164-70.
39. Lovell, S.C.; Davis, I.W.; Arendall, III W.B.; De Bakker, P.I.; Word, J.M.; Prisant, M.G.; Richardson, J.S.; Richardson, D.C., *Proteins.*, **2003**, 50(3), 437-50.
40. BIOVIA: Materials Studio 8.0, Dassault Systemes Biovia, Cambridge, UK, **2015**.
41. Leeson, P., *Nature.*, **2012**, 481(7382), 455-6.
42. Trott, O.; Olson, A. J. *J Comput Chem.*, **2010**, 31(2), 455-61.
43. Morris, G.M.; Huey, R.; Lindstrom, W.; Sanner, M.F.; Belew, R.K.; Goodsell, D.S.; Olson, A. J. *J Comput Chem.*, **2009**, 30(16), 2785-91.
44. Lim, S.V.; Rahman, M.B.; Tejo, B.A *BMC Bioinform.*, **2011**, 12(13), 1-12.
45. Jaghoori, M.M.; Bleijlevens, B.; Olabariaga, S.D. *J. Comput. Aided Mol. Des.*, **2016**, 30, 237-49.
46. Glantz-Gashai, Y.; Meirson, T.; Samson, A.O., *PLoS Comput. Biol.*, **2016**, 12(12), e1005293.
47. Lipinski, C.A.; Lombardo, F.; Dominy, B.W.; Feeney, P. *J. Adv. Drug Deliv. Rev.*, **2012**, 64, 4-17.
48. Seeliger, D.; de Groot, B.L., *J. Comput. Aided Mol. Des.*, **2010**, 24(5), 417-22.
49. Nguyen, T.H.; Zhou, H.X.; Minh, D.D. *J. Comput. Chem.*, **2018**, 39(11), 621-36.
50. Saxena, P.; Mishra, S., *Int. J. Pept. Res. Ther.*, **2020**, 26(4), 2437-48.